F_2 against DGLAP *

Dieter Haidt
Deutsches Elektronensynchrotron DESY
22603 Hamburg
E-mail: dieter.haidt @ desy.de

The properties of the DGLAP kernels are tested using the structure function F_2 in the low-x regime.

1 Introduction

The structure function data obtained both in neutrino and charged lepton fixed target experiments have established the validity of the DGLAP evolution equations at next-to-leading order QCD. The two HERA experiments H1[1] and ZEUS[2] have extended these measurements into the considerably enlarged phase space accessible at the HERA ep-collider. In the valence region values of Q^2 up to 20 000 GeV^2 are probed and in the low Q^2 region values of x down to 10^{-6}. The latter region is particularly interesting, because now the low-x properties of the DGLAP kernels can be probed, while still remaining at $Q^2 > 1$ GeV^2, i.e. in the region dominated by perturbative physics. Using the variable $q = \log(1 + Q^2/Q_0^2)$ with fixed Q_0^2=0.5 GeV^2 instead of ln Q^2 it is possible to display simultaneously low and high Q^2 data and to examine the behaviour of F_2 near $Q^2 = 0$ [3]. In the deep sea, defined by x <0.001, the F_2^{ep} data behave approximately linearly in q. Fig. 1 (left) shows the data in an x-bin centered at 10^{-4} together with the prediction of the global fit by MRST[5] starting at Q_{st}=1.25 GeV^2, i.e. $q_{st} = 0.55$. Although the fit is good, its shape exhibits a positive curvature as opposed to the flat behaviour of the data. 2-parameter fits in q are carried out to both the F_2 data and the corresponding values predicted by the MRST-parametrization. The quadratic term, i.e. the curvature, is displayed in Fig. 1 (right) and shows a trend not supported by data. It is the aim of this study to relate this systematic deviation to features of the DGLAP kernels at low x.

*Talk held at DIS03, St.Petersbug, April 22,2003; an elaborated version is in progress.

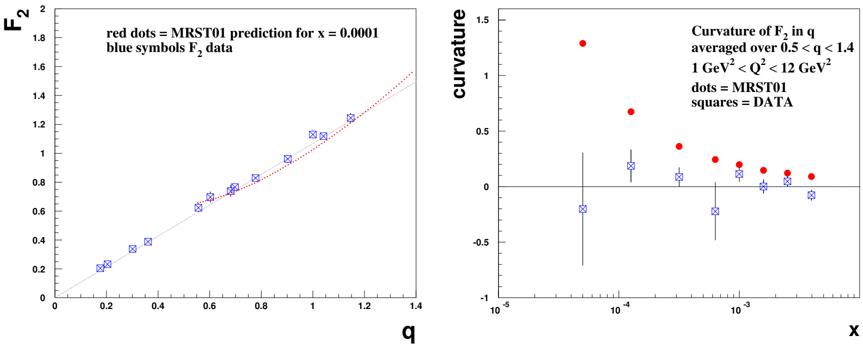

Figure 1: Left: Measured structure function $F_2(10^{-4}, q)$ vs. q compared with MRST prediction (dotted curve). Right: The curvature of F_2 w.r.t. q in bins of x for data (crosses) and MRST (dots).

2 Method

The second derivative of F_2^{ep} w.r.t. q, $\partial_q^2 F_2^{ep}$, is predicted at fixed q assuming the validity of the DGLAP equations and compared with data from the HERA experiments. The method is worked out in the perturbative region at $q = 1$ and applied to the region 0.00001< x <0.001, thus probing specifically the low-x structure of the DGLAP kernels.

3 Decomposition of F_2^{ep}

Eq. 1 shows the standard decomposition of F_2 in ep scattering (see ref.[4]) suitable for the Q^2-evolution in QCD.

$$F_2^{ep} = C_F \otimes N + \epsilon\,(C_F \otimes Q^+ + C_G \otimes G) \tag{1}$$

The meaning of the quantities is:

- Coefficient functions : C_F and C_G
- Parton distribution functions $q_i, \overline{q}_i, g$ are combined to form a Singlet: $Q^+ = \sum_i^f x(q_i + \overline{q}_i)$ with f active flavors, a Nonsinglet: $N = \sum_i^f \left(e_i^2 (x(q_i + \overline{q}_i) - \frac{1}{f}\, Q^+) \right)$ and Gluon : $G = xg$

- $\epsilon = \frac{1}{f}\sum_i^f e_i^2$ (e_i=QED coupling constants for flavor i)

The singlet contribution ϵQ^+ dominates F_2^{ep}. Its evolution is determined by the coupled DGLAP equations involving also the gluon distribution function (short hand $\partial_q = \partial/\partial q$) :

$$\partial_q \begin{pmatrix} Q^+ \\ G \end{pmatrix} = a(q) \begin{pmatrix} P_{qq} & P_{qg} \\ P_{gq} & P_{gg} \end{pmatrix} \otimes \begin{pmatrix} Q^+ \\ G \end{pmatrix} \tag{2}$$

where $a(q)$, due to the variable change from ln Q^2 to q, is given by :

$$a(q) = \frac{\alpha_s(Q^2)}{2\pi} \frac{Q^2 + Q_0^2}{Q^2} \ln 10$$

The kernels in eq. 2 are used at next-to-leading order (see ref. [4]). A striking feature of all kernels at next-to-leading order is the presence of $1/x$ terms. Fig. 2 illustrates the rise of the off-diagonal kernels P_{qg} and P_{gq} for x <0.001.

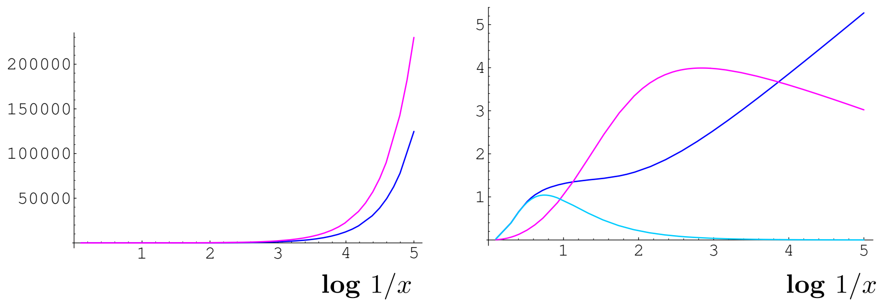

Figure 2: Left: P_{gq} (upper curve) and P_{qg} vs log $1/x$. Right: The distributions $Q^{\pm}$ and G at $q = 1$ vs log $1/x$.

4 Evaluation of $\partial_q^2 Q^+$

The second derivative of the singlet Q^+ is obtained by differentiating the 1^{st} DGLAP equation w.r.t. q :

$$\partial_q Q^+ = a(q) P_{qq} \otimes Q^+ + a(q) P_{qg} \otimes G \tag{3}$$

and has the form : $\partial_q^2 Q^+(x,q) = (Quark - term) + (Gluon - term)$. The quark term is small, since Q^+ is approximately proportional to q and $qa(q)$ is only weakly q-dependent (see also Fig. 3). On the contrary, the gluon term consisting of three contributions

$$aP_{qg} \otimes G \cdot \left(\frac{a'}{a} + \frac{\alpha_s'}{\alpha_s} - \frac{\alpha_s'}{\alpha_s} \frac{P_{qg}^{LO} \otimes G}{P_{qg} \otimes G} + \frac{P_{qg} \otimes \partial_q G}{P_{qg} \otimes G} \right)$$

generates a strong x-dependence in the deep sea, which is caused by the occurrence of the gluon in form of $\partial_q G$ in the numerator and G in the denominator. Substituting for $\partial_q G$ the second DGLAP equation (see eq. 2) $P_{qg} \otimes P_{gg} \otimes G$ dominates the x dependence. The numerical evaluation of $\partial_q^2 Q^+$ as a function

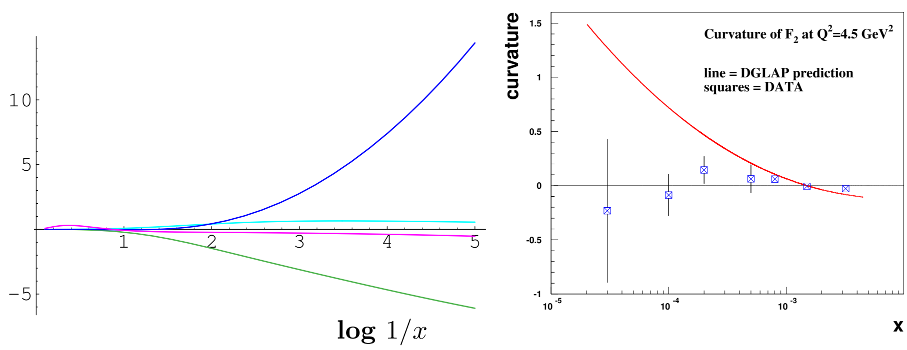

Figure 3: Left: Contributions to $\partial_q^2 Q^+$: the curves from top to down are gluon term 3,2, quark term and gluon term 1 vs log $1/x$. Right: Predicted and measured curvature of F_2^{ep} vs. x for fixed $q = 1$.

of x for $q = 1$ requires the knowledge of two input functions: Q^+ and $\partial_q Q^+$ are set to ϵ times the measured F_2^{ep} and $\partial_q F_2^{ep}$. This is a good approximation, since the nonsinglet is small compared to ϵQ^+ and $C_F \otimes Q^+ = Q^+ + \mathcal{O}(\alpha_s/2\pi)$. The gluon is determined using eq. 3 as constraint. The result is shown in Fig. 3(left) for $q = 1$.

5 Prediction of $\partial_q^2 F_2^{ep}$

Eq. 1 must be differentiated twice w.r.t. q. The r.h.side is dominated by $\partial_q^2 Q^+$ and gets $\mathcal{O}(10\ \%)$ contributions from the known coefficient functions mainly through it application to the gluon. The effect of the non-singlet is negligible.

6 Conclusions

The predicted curvature of F_2^{ep} in q is compared in Fig. 3(right) with the measured one. The low-x discrepancy is caused by specific features (the $1/x$ terms) in the DGLAP kernels and cannot be attributed to the parton distribution functions.

In the $\overline{MS}$ scheme the NLO contributions are numerically equally important as the leading ones as soon as x is in the deep sea.

Acknowledgements

I like to thank Prof. L. Lipatov for the invitation to St.Petersburg and the convenors for the lively discussions. I enjoyed fruitful discussions with Profs. J. Bartels, Yu. Dokshitzer, T. Gehrmann, H. Spiesberger and P. Zerwas.

References

[1] [H1] C. Adloff et al.: Nucl.Phys.**B497** (1997) 3-30; S. Aid et al.: Nucl.Phys.**B470** (1996) 3-40; T. Ahmed et al.: Nucl.Phys.**B439** (1995) 471-502; hep-ex/0304003

[2] [ZEUS] J. Breitweg et al.: Phys.Lett.**B487** (2000) 53 (BPT); J. Breitweg et al.: Phys.Lett.**B407** (1997) 432 (BPC); M. Derrick et al.: Z.Phys.**C69** (1996) 607; J. Breitweg et al.: Eur.Phys.J.**C7** (1999) 609 (SVX); S. Chekanov et al.: Eur.Phys.J.**C21** (2001) 443;

[3] D. Haidt, *DIS97* Chicago, April 1997, AIP Conference Proceedings 407 (1997) 386.

[4] W. Furmanski and R. Petronzio, Z.Phys. **C11** (1982) 293-314.

[5] A.D. Martin et al., Eur.Phys.J **C23** (2002) 73.